Astron. Astrophys. 306, 212–218 (1996)

ASTRONOMY AND ASTROPHYSICS

# A wind in the intermediate polar candidate 1 H0551-819?*

**M. Mouchet[1,2], L. Siess[3], J. Drew[4], J.P. Lasota[5], D.A.H. Buckley[6], and J.M. Bonnet-Bidaud[7]**

[1] DAEC, Unité associée au CNRS et à l'Université Denis Diderot, Observatoire de Paris, Section de Meudon, F-92195 Meudon Cedex, France
[2] Université Denis Diderot, Place Jussieu, F-75005 Paris, France
[3] Laboratoire d'Astrophysique, Observatoire de Grenoble, B.P.53X, F-38041 Grenoble Cedex, France
[4] Department of Physics, Keble Road, Oxford, OX1 3RH, UK
[5] Unité propre 176 du CNRS, DARC, Observatoire de Paris, Section de Meudon, F-92195 Meudon Cedex, France
[6] South African Astronomical Observatory, PO Box 9, Observatory 7935, Cape Town, South Africa
[7] CEA, DSN/DAPNIA/Service d'Astrophysique, CEN Saclay, F-91191 Gif sur Yvette Cedex, France

Received 5 December 1994 / Accepted 12 May 1995

**Abstract.** IUE observations of the cataclysmic variable 1 H0551-819 obtained at three different epochs reveal P-Cygni type profiles in the CIV line. The shape of these profiles is modulated with the orbital period of the system. The observations suggest the presence of a wind in the system. We considered several models of wind, disc and continuum emitting hotspot that could account for the orbital modulation of the line profiles but none of them gave satisfactory results.

**Key words:** stars: cataclysmic variables – stars: individual 1 H0551-819 – X-rays: stars – accretion

## 1. Introduction

The X-ray source 1 H0551-819 has been optically identified by Buckley et al. (1993, hereafter B93) with a blue cataclysmic variable showing strong emission lines. The moderate intensity of the HeII 4686Å line compared to $H_\beta$ and the hard X-ray flux has led B93 to classify this source as a possible Intermediate Polar (IP). These systems are a sub-class of cataclysmic binaries, consisting of a magnetic white dwarf which accretes matter from a late type star filling its Roche lobe (see reviews by Berriman 1988 and Patterson 1994). The rotation of the white dwarf at a period $P_{\rm spin}$ is faster than the orbital motion: for most confirmed IPs the ratio of periods is close to 0.1. (King & Lasota 1991, Warner & Wickramasinghe 1991). The X-ray and optical fluxes are modulated at both spin ($P_{\rm spin}$) and orbital ($P_{\rm orb}$) periods as well as at their orbital sideband, or beat, periods (Warner 1986, Hellier 1991). The presence of an accretion disc around the white dwarf in IPs is still debated (King & Lasota 1991, Hellier 1991, Buckley et al. 1995).

Optical photometric data of 1 H0551-819 have revealed a period of 3.34h which has been confirmed to be the orbital one from radial velocity data (B93). Variability on different timescales is also present, in particular quasi-periodic oscillations with periods of 1781s and 1390s have been occasionally detected but it is difficult to identify them with coherent spin or beat periods. The periodic spin related pulsations might be hidden by the large degree of flickering in the system. Therefore 1 H0551-819 cannot be unambigously classified as an IP.

We have undertaken a systematic study of UV spectra of intermediate polars in order to provide a complete energy budget from X-rays to the optical/IR. In this framework we have observed 1 H0551-819 with IUE and discovered atypical emission line profiles. An indication of a P-Cyg profile is found in some spectra. Such profiles are observed in different kinds of cataclysmic variables (dwarf novae in outburst, novalike systems) and are thought to be associated with the presence of a wind (see recent reviews by Drew & Kley 1993, Cordova 1995).

## 2. Observations and data reduction

1 H0551-819 was observed with the IUE satellite on Apr. 22 1990, Apr. 16 and Nov. 08 1991 in the low resolution (6Å) mode and with the large aperture (10"x20") in both SWP ($\lambda\lambda 1150-1950$) and the LWP ($\lambda\lambda 1950-3250$) cameras. The nearby star at 3" of spectral type K0 (B93) was thus also included in the aperture. The log of observations is reported in Table 1. Orbital phases have been computed using the ephemeris given by B93. Phase 0 corresponds to the time of the optical photometric maximum. The accuracy of this ephemeris leads to an uncertainty of up to 0.05 for the furthest Nov. 91 spectra. The exposure times were chosen to be near multiples of 24 minutes, close to

*Send offprint requests to*: M. Mouchet; e-mail: mouchet@obspm.fr

* Based on observations made with the International Ultraviolet Explorer, collected at the Villafranca Satellite Station of the European Space Agency.

**Table 1.** Log of the IUE observations

| IUE Image N° | mid.exp. HJD(244+) | exp. time (min.) | $\phi$ | V (FES) |
|---|---|---|---|---|
| | April 22 1990 | | | |
| SWP 38644 | 8003.57761 | 24 | 0.66 | 13.46 |
| LWP 17784 | 8003.60096 | 24 | 0.84 | 13.34 |
| SWP 38645 | 8003.62432 | 24 | 0.01 | 13.55 |
| LWP 17785 | 8003.65900 | 24 | 0.26 | 13.55 |
| SWP 38646 | 8003.68499 | 24 | 0.45 | 13.73 |
| LWP 17786 | 8003.70899 | 24 | 0.62 | 13.46 |
| SWP 38647 | 8003.73986 | 48 | 0.84 | 13.38 |
| LWP 17787 | 8003.77093 | 24 | 0.06 | 13.46 |
| SWP 38648 | 8003.80820 | 46 | 0.33 | 13.59 |
| LWP 17788 | 8003.83717 | 23 | 0.54 | 13.66 |
| SWP 38649 | 8003.85892 | 22 | 0.70 | 13.42 |
| | April 16 1991 | | | |
| LWP 20158 | 8362.79807 | 24 | 0.91 | 13.40 |
| SWP 41399 | 8362.84113 | 75 | 0.22 | 13.68 |
| | November 08 1991 | | | |
| SWP 43037 | 8568.70032 | 48 | 0.47 | |
| LWP 21666 | 8568.74016 | 48 | 0.75 | 13.96 |
| SWP 43038 | 8568.77109 | 28 | 0.98 | 15.19 |

one of the possible spin periods. The UV spectra have been reduced manually from two-dimensional images. They have been checked for correct centering and for spurious defects, in particular around the CIV line. The extracted spectra have been compared with one-dimensional calibrated spectra obtained by the automatic standard procedure: IUESIPS, at VILSPA. No significant differences have been found. The degradation of the camera sensitivity between April 90 and Nov. 91 is less than 1.3% for SWP and 2.2% for LWP (Garhart 1992). Fine Error Sensor (FES) measurements were acquired before each spectrum exposure. In April and Nov. 91 the new reference point in the FES field has been used. In Nov. 91 only two measurements could be done because of the bright level of the background due to scattered light. The V magnitude was computed using the calibration derived by Barylak (1990) for the April 90 data and by Perez (1991) for April and Nov. 91. No correction due to the focus was taken into account, which leads to a maximum error of 0.02 mag. Since the size of the field of view includes the contribution of the nearby star, a colour correction ($B-V=0.27$, B93) was applied. The resulting V magnitude, after subtracting the contribution of the companion, is reported in Table 1 with an estimated accuracy of 0.05. The Nov 91 FES measurements contaminated by scattered light correspond to a very low optical brightness level of the source, not confirmed in the UV, and thus will be disregarded. The typical V value is quite consistent with previous optical measurements (B93).

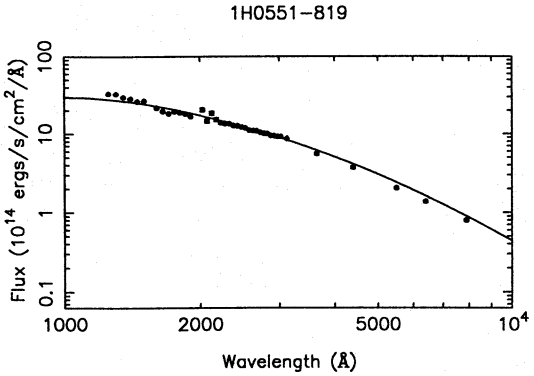


**Fig. 1.** Dereddened averaged energy distribution. The UV data are from the average SWP+LWP spectrum and UBVRI data are from B93. The best blackbody disc model fit is reported (see text for the corresponding parameters). Note the excess at short wavelengths

## 3. UV continuum

### *3.1. Mean spectrum and reddening*

Since the source did not exhibit any strong changes in the UV during the three epochs of observations (see below), an average spectrum in each wavelength range has been produced. In the short wavelength range it mainly shows emission lines of SiIV and CIV superimposed on a blue continuum, while at long wavelengths the MgII line, often observed in emission in cataclysmic variables, is very weak. To study the energy distribution, the UV flux has been averaged into 50Å intervals. Only the wavelengths in regions free of lines have been used. Error bars for each measurement at a given UV wavelength correspond to the errors on the mean flux within the 50Å band and thus do not reflect the deviation between the 9 SWP or 7 LWP spectra which have been averaged. Although no strong reddening is immediately apparent around 2200Å, an eye-estimate, based on plots of a grid of dereddened continua from 0.05 to 0.19 with a step of 0.02, leads to a plausible reddening value in the range 0.09 to 0.15. A fit of the average SWP+LWP continuum, with a reddened power law (Seaton 1979) which is assumed to be the envelope of an 'ideal' un-blanketed continuum, gives a value of $E_{B-V}=0.12$ with a slope $\alpha=-1.42$ ($F_\lambda \sim \lambda^\alpha$) but this result, corresponding to a minimum reduced $\chi^2$ of 16.9, is formally not acceptable. A reddening value of 0.12 will be assumed in the following. It is lower than, and hence compatible with the HI interstellar measurements by Burstein & Heiles (1982) in the direction of the source ($0.15 < E_{B-V} < 0.18$). Using an average absorption of 1.6 mag/kpc (Allen 1973) yields a distance of 230 pc. Though very uncertain, this distance estimate falls within the distance scale of the K dwarf population computed in the direction of 1 H0551-819 from the galactic disc scale height derived by Kuijken & Gilmore (1989).

In keeping with the line profile synthesis study (see Sect. 5), the average energy distribution from the UV to the optical (UBVRI) has been formally fitted with a standard blackbody accretion disc model (Frank et al. 1992), neglecting all other possible contributions such as the secondary, the white dwarf, a possible gas stream and hot spots. An average V magnitude of 13.51 obtained from the thirteen reliable FES values and colours derived by B93 have been used. The error bars are determined from the error on the average V magnitude. We note that the optical fluxes are in agreement with the UV distribution. The model is parameterized by a characteristic temperature $T_*=(3GM\dot{M}/8\pi\sigma)^{0.25}R_1^{-0.75}$, the outer to inner disc radius ratio $R_0/R_1$ and C the normalization factor ($C=(4\pi hc^2)\cos i\, R_1^2/d^2$). Here $M$ and $\dot{M}$ are respectively the white dwarf mass, the accretion rate, and $i$ the inclination angle. The best fit, plotted in Fig. 1, is obtained for the following parameters : $R_0/R_1$= 27, $T_*$ = 77000 K, C=4.2 $10^3$ erg $cm^{-2}s^{-1}$ but it is however formally not acceptable (reduced $\chi^2$=44.1). The outer to inner disc ratio is expected to be smaller if the contribution of the companion would have been taken into account. If the disc fills 90% of the white dwarf Roche lobe, the inner radius corresponds to 1.2 $R_{wd}$, assuming a main sequence red star filling its Roche lobe and a typical white dwarf mass of 0.6 $M_\odot$. An accretion rate of 5 $10^{-9}$ $M_\odot$/yr and an upper limit for the distance of 360 pc are then derived. However, an excess in the observed flux with respect to the model remains at short UV wavelengths. This could be attributed to a heated white dwarf (T $\sim$ 85000K). However steady-state blackbody disc models generally fail to account for the energy distribution of cataclysmic variables. Moreover the brightness temperature-radius profiles derived from eclipse-mapping studies of some novalike variables appear to be flatter than expected from a steady-state disc (Rutten et al. 1992). Models synthesised from plane-parallel stellar atmospheres do not give satisfactory fits either (Wade 1988) and are not applicable for various reasons as discussed by Hubeny (1990). No theory of the vertical structure of a stationary accretion disc has yet achieved widespread acceptance. The approach of Shaviv & Wehrse (1991) leads to a good agreement of their models with the energy distribution of some novalikes over a large energy range. In particular, as is true also of stellar atmosphere models (Wade 1984), they predict a flux increase at short wavelengths which is not observed in the blackbody disc model of the same accretion rate. If such models are appropriate, they would eliminate the need to invoke an additional flux component due to the white dwarf or a boundary layer. In any case, the UV energy distribution does not seem to require the presence of an extended hole in the accretion disc (see Sect. 5.2).

### *3.2. Orbital modulation*

In Fig. 2, continuum fluxes at 1450Å and 2650Å, measured in individual spectra, are shown versus orbital phase, as well as the optical flux derived from the FES (Nov. 91 excluded). Error bars for the UV fluxes correspond to the error of the mean flux within the 50Å band, while a typical error value of 0.05 mag for the V magnitudes derived from the FES was estimated. Different symbols are attributed for data obtained at different epochs. The contribution of the nearby K0 star is negligible at these two specific UV wavelengths. The UV and optical fluxes show variations at the orbital period as well as long-term changes. We note that the SWP continuum of the April 1991 long exposure (75 min.) spectrum exhibits the highest value, while the corresponding LWP flux and V measurements have more typical values. Also the total SWP flux (1230-1950Å) and LWP flux (1950-3200Å) have been measured and they exhibit the same behaviour as fluxes at 1450Å and 2650Å respectively. The flux modulation has been fitted for the April 1990 data only, assuming a sinusoidal shape. The amplitudes and maximum phases of the modulation are 10.1 $\pm$ 1.1%, 17.6 $\pm$ 0.7%, 14.4 $\pm$ 2.2% and 0.658 $\pm$ 0.013, 0.908 $\pm$ 0.005, 0.791 $\pm$ 0.022 respectively for 1450Å, 2650Å and the V magnitude, with corresponding minimum reduced $\chi^2$ of the fit of 1.56, 21.7 and 2.13 (error bars at $1\sigma$ level). The optical flux measured with the FES is not at maximum at the expected phase 0.0 (maximum uncertainty due to the present accuracy of the orbital period of 0.05) and the amplitude is larger than that derived from the average optical light curve fitted by B93 (4.5%), but large fluctuations have been observed (B93) from one cycle to the next. These fluctuations may explain the discrepancy in phase, although if present such scatter would also distort the shape of the modulation. Contrary to the FES measurements which are acquired in a short time (less than one minute), the SWP and LWP fluxes cover tens of minutes typically, and thus could be less affected by flickering if present in the UV.

## 4. Line profiles

In Fig. 3, SWP spectra are plotted in order of increasing phase. Clear changes are observed in line profiles. Between phases 0.84 and 0.22 a blue absorption feature is present in the CIV line while the SiIV doublet is hardly detectable. Around phase 0.5 the CIV and SiIV profiles are observed in emission. These four spectra have been obtained during the three observation epochs. This repeatability of this behaviour on a timescale of 1.5 years confirms the accuracy of the orbital period. In addition, strong absorption at 1300Å is present in all spectra, which is identified as a SiIII line. The profiles of the NV line, close to the geocoronal $L_\alpha$ line and to the SiII 1260Å absorption line, are badly defined. The blue absorption component seen in the CIV line is clearly reminiscent of a P-Cygni profile. Since the signal-to-noise ratio of individual spectra is low we have produced a typical CIV profile for phases 0 and 0.5 by averaging the three less noisy spectra: SWP 41399, 38645, 38647 and SWP 38644, 38648, 43037, respectively. At phase 0.0 the resulting profile exhibits a blue narrow absorption while at phase 0.5 it is characterized by a pure, slightly asymmetric emission. The best gaussian fit to this emission is centered at 1549.6Å , with a full width at half maximum of the order of 2100 km/s. The slight difference in the width and in the position between the three individual profiles which compose the average one cannot account for this large width value.

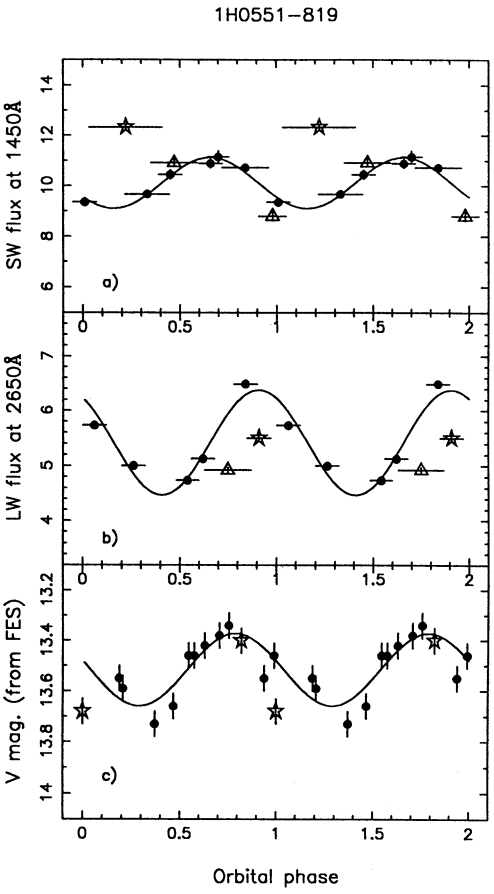


**Fig. 2a–c.** The orbital modulation of continuum flux at 1450Å(**a**), 2650Å (**b**) and in V (derived from FES measurements) (**c**). Data in Apr. 90 (dots), in Apr. 91 (open stars) and in Nov. 91 (open triangles) are shown. The sinusoidal curves are the best fits on April 90 data. Data are shown twice for clarity. Horizontal bars represent the extension of the exposures

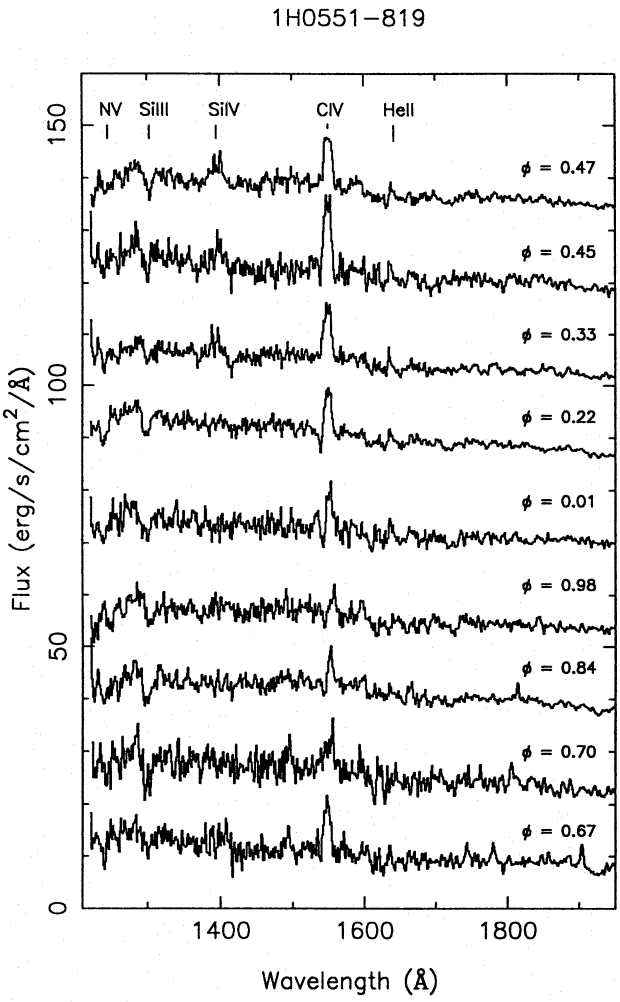


**Fig. 3.** The CIV profiles of individual spectra in order of increasing orbital phase. An absorption component is detectable between phase 0.84 and 1.22

## 5. Wind model

### *5.1. Description*

In order to form an impression as to what may give rise to the variable CIV profiles, we have made comparisons with theoretical profiles synthesized using a recently-adapted version of the code first presented by Drew (1987). Basically the wind code produces normalized line profiles on the assumption that the underlying continuum is due to the sum of an accretion disc radiating according to a standard blackbody model (Frank et al. 1992) and a white dwarf, also radiating as a blackbody. The white dwarf temperature is for the present purpose derived from the fraction of the accretion luminosity not radiated in the disc. The wind ionization is assumed to be constant (in effect the model parameter determining the number density of scattering ions is proportional to $\dot{M}q$, where $\dot{M}$ is the total mass loss rate, and $q$ is the scattering ion fraction – a quantity that in principle may vary with position). The wind velocity increases linearly with distance from the white dwarf out to a radius $R_\infty$, beyond which it is held constant and equal to $v_\infty$.

It is suspected that the white dwarf may have a strong enough magnetic field to disrupt the inner accretion disc. If this is so, it is even more of a problem than usual to select an outflow geometry. We have tried the following simple model. The outflow is assumed to be bipolar, with its symmetry axis parallel to that of the disc. The density distribution varies as $(cos\theta)^l$ where $l$ is the so-called bipolarity index. Even if it were the case that the outflow axis tracks the white-dwarf spin axis, our assumption of coalignment with the disc axis in effect allows for the 'smearing' we can expect – given that each SWP exposure spans almost a complete spin period or longer. The model ingredients thus far cannot yield synthetic line profiles that change with orbital phase. There has to be some departure from axisymmetry within the UV bright system. Since we have seated the outflow in the centre of the disc, which could only plausibly lead to variability on the white dwarf spin period or similar, we have no option but to locate the departure from axisymmetry in the accretion disc. The observed orbital phase variation of the line profiles is then attributable to disc 'structure' that passes behind and is shad-

owed by the outflow once each binary orbit. For simplicity, we take this structure to be a small 'spot' emitting continuum light only (cf. the similar approach used by Prinja, Drew & Rosen 1992).

The following model parameters were held fixed: the white dwarf mass was set at the typical value of $M_{wd}$ = 0.6 $M_\odot$; on applying the mass-radius relation of Nauenberg (1972) this in turn fixes $R_{wd}$ = 8.7 $10^8$ cm; the outer disc radius used was $R_{ext}$ = 2.6 $10^{10}$ cm (0.87 of the white-dwarf Roche lobe radius if the companion is a Roche-lobe filling main sequence star). The size and temperature of the continuum-emitting hotspot were chosen such that it contributed 31% of the total monochromatic continuum flux at ~1550 Å. An accretion rate of 5 $10^{-9}$ $M_\odot$ $yr^{-1}$ was chosen in order to achieve consistency with the blackbody disc model for the energy distribution.

### 5.2. Results

The closest fits found to the $\phi$ = 0.0 and $\phi$ = 0.5 mean observed profiles are shown in Fig. 4. The computed profiles have been smoothed to a spectral resolution of 6 Å, to facilitate comparison with low dispersion IUE data. The parameters of the model yielding these profiles are listed in Table 2. These fits are clearly unsatisfactory. We note that the choice of the accretion rate value, strongly dependent on the underlying accretion disc model, does not affect this conclusion. There are two reasons why these model profiles are unsatisfactory. First, it was found necessary to adopt a disc inner radius as large as $10R_{wd}$ in order to reproduce the observed emission-dominated profiles, while a much lower value $\sim 1.2R_{wd}$ is derived from the blackbody disc fit to the energy distribution. This, of course, is a direct contradiction. We are not in a position to comment precisely on how different the result might have been if the disc continuum at ~1549Å had been calculated following the methods of Wade (1988) or Shaviv & Wehrse (1991). But it is clear that these prescriptions would have had to have allowed a large central hole in the disc in order to avoid this problem, and yet it seems unlikely that at the same time the observed energy distribution could be matched. In addition, and somewhat implausibly, the disc hotspot needed to introduce the orbital phase variation had to be positioned right at the inner edge of the disc to achieve maximum scattering of its light by the wind, and hence maximum phase contrast. Second, the basic ingredients of the model always combine to produce blueshifted absorption extending to higher velocities than the emission that replaces it around the other side of the orbit.

Similar problems were encountered by Prinja, Drew & Rosen (1992) who modelled the UV resonance lines in the spectrum of V795 Her in much the same way. They proposed that one of the ways to improve the model was to postulate the presence of a 'disc hotspot' that produces line rather than continuum emission. In the case of 1 H0551-819 this type of model seems to be even more appropriate. A 'background' source of line emission would be covered, over some fraction of the binary orbit, by 'cold' outflowing material. Unfortunately, our data quality is not good enough to allow an attempt at modelling this.

**Table 2.** Wind model parameters

| | |
|---|---|
| mass loss rate $\dot{M}$ | $10^{-10}$ $M_\odot$ $yr^{-1}$ |
| terminal velocity $v_\infty$ | 2500 km $s^{-1}$ |
| radius $R_\infty$ | 40 $R_{wd}$ |
| wind temperature | 50000 K |
| bipolarity $l$ | 20 |
| inclination | 53° |
| hotspot temperature | 70000 K |

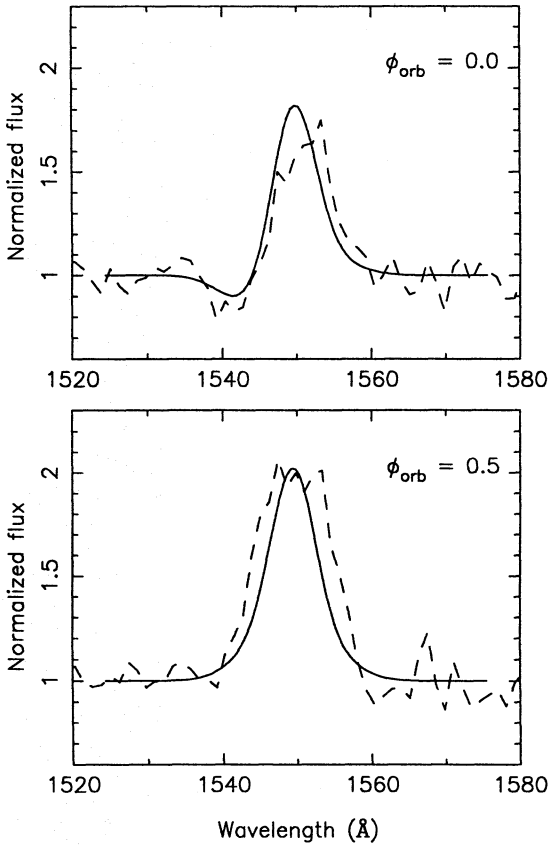


**Fig. 4.** Best wind model fit for profiles close to phase 0 (top) and phase 0.5 (bottom). Corresponding parameters are given in the text

## 6. Discussion

While the UV continuum shape of 1 H0551-819 is typical of the class of IPs (Bonnet-Bidaud & Mouchet 1988) its line behaviour differs from most of these objects. In addition to the absorption component observed at specific phases in the CIV line the spectra do not show a strong He II line while the optical HeII 4686Å is clearly detected (B93), albeit weakly compared to most IPs. We now compare the orbital UV modulation in 1 H0551-819 with those observed in known IPs, and discuss the existence of a wind.

### 6.1. Continuum orbital modulation

The analysis of the continuum modulation at a specific wavelength or on a wider wavelength range provides tentative evidence that the continuum flux at short UV wavelengths is out of phase with the optical flux, while it is nearly in phase at long wavelengths. Similar behaviour is observed to a lesser extent in the intermediate polars FO Aqr (de Martino et al. 1994) and BG CMi (de Martino et al. 1995). By analogy with the optical modulation observed in AO Psc, B93 conclude that in 1 H0551-819 the white dwarf is in front of the secondary at phase 0.0. This requires that the radial velocity of the emission lines is attributable to the hotspot, though no S-wave is present in the optical line profiles. However the spectral data set reported in B93 are rather limited. The relative UV and optical phasing is in agreement with the explanation proposed by de Martino et al. (1994, 1995) for the orbital UV-optical modulation, requiring two distinct X-ray illuminated regions: one identified with the heated hemisphere of the secondary star, and the other with a hot, vertically extended structure on the disc close to the white dwarf, possibly a result of the accretion stream overflowing the disc (Lubow 1989). This hotspot should be displaced from the line of centres in order to account for the phase shift between the far UV and the optical.

### 6.2. Presence and geometry of the wind

P-Cygni profiles have often been observed in non-magnetic cataclysmic variables but only one IP (TV Col) clearly shows such profiles during normal quiescent states (Bonnet-Bidaud et al. 1985) and during mini-outbursts (Mateo et al. 1985) (Note that AO Psc also shows indications of an absorption component (Drew 1991)). Moreover TV Col is also similar to 1 H0551-819 in that its spin period (33 min.) is not yet detected in optical photometry. V795 Her, which also exhibits P-Cygni profiles, was suggested to be an IP but this is not yet confirmed by any X-ray observations (Prinja & Rosen 1993). The presence of a wind is directly related to high accretion rates as are present in dwarf novae during outbursts and in novalike systems. However, for IPs, because of their high magnetic field and strong X-ray flux, the physical conditions for producing such a wind might be altered.

Apart from eclipsing systems, variations on a timescale of a few hours in the CIV wind profiles have been observed in several CVs (Drew 1993) and in the IP TV Col (Bonnet-Bidaud et al. 1985). These variations are orbitally modulated in most cases (Woods et al. 1990, 1992, Drew & Verbunt 1988). In V795 Her these variations are periodic but with a period (P=4.86h) quite different from the optical spectroscopic period (2.60h) (Prinja et al. 1992, Prinja & Rosen 1993). A range of alternative explanations of this modulation has been mooted in the past: specifically, modulation due to an additional continuum contribution, such as from a disc hotspot (Woods et al. 1992, Prinja et al. 1992), an inclined bipolar wind (Drew & Verbunt 1988, Prinja et al. 1992), or an additional asymmetric emission line component (Prinja et al. 1992, Knigge et al. 1994). Objections have been raised against all but the last possibility.

In 1 H0551-891, we have tried, with no success, to reproduce the absorption component observed at phase 0.0 by adding a hotspot at the inner disc rim, which should be situated behind the white dwarf, at that point in the orbit, to account for the most prominent blueshifted absorption. However any source of line emission coming into view at specific phases and conveniently superposed on the spectrum can fill in this blueshifted absorption.

## 7. Conclusion

On the basis of its UV properties, 1 H0551-819 cannot be firmly related to the class of intermediate polars although one source of this class, TV Col, shows similar properties, in particular the presence of P-Cygni profiles in the CIV line. Moreover it is striking that this line profile is modulated with the orbital period as for TV Col. No simple wind model can reproduce the shape of the profiles observed at the two opposite phases, 0.0 and 0.5. However high temporal resolved UV spectra at high signal-to-noise ratio are necessary to confirm the existence of a wind and the origin of the asymmetry.

*Acknowledgements.* We thank Didier Pelat for valuable discussions on statistical methods and the referee Frank Verbunt for helpful comments on the first manuscript

## References

Allen, C.W., 1973, "Astrophysical Quantities", Athlone Press, London
Barylak M., 1990, IUE ESA Newsletter 34, 26
Berriman G., 1988, in "Polarized Radiation of Circumstellar Origin", Vatican Press, p.281
Bevington P. R., 1969, "Data Reduction and Error Analysis for the Physical Sciences", Ed. McGraw-Hill Book Company
Bonnet-Bidaud J.M., Mouchet M., 1988, in "A Decade of UV Astronomy with the IUE satellite" ESA SP-281, p.271
Bonnet-Bidaud J.M., Motch C., Mouchet M., 1985, A&A 143, 313
Buckley D.A.H., Remillard R.A., Tuohy I.R., Warner B., Sullivan D.J., 1993, MNRAS 265, 926 (B93)
Buckley D.A.H., Sekiguchi K., Motch C., et al., 1995, MNRAS in press
Burstein D., Heiles C., 1982, AJ 87, 1165
Cassatella A., Gonzalez-Riestra R., Oliversen N., Lloyd C., 1992, A&A 256, 320
Cordova F.A.D., 1995, in "X-ray Binaries", eds W.H.G. Lewin, J. van Paradijs, E.P.J. van den Heuvel, in press
de Martino D., Buckley D., Mouchet M., Mukai K., 1994, A&A 284, 125
de Martino D., Mouchet M., Bonnet-Bidaud J.M. et al., 1995, in press
Drew J.E., 1987, MNRAS 224, 595
Drew J.E., 1991, in "Structure and Emission Properties of Accretion Disks", 6th IAP Astrophysics Meeting, IAU Coll n°122, eds C. Bertout, S. Collin-Souffrin, J.P. Lasota, J. Tran Thanh Van, Eds Frontières, p.331
Drew J.E., 1993, in "Cataclysmic Variables and Related objects", Eds O. Regev and G. Shaviv, Annals of the Israel Physical Society, vol.10, p.128

Drew J.E., Kley W., 1993, in "Accretion disks in compact stellar systems", ed. J.C. Wheeler, Advanced Series in Astrophysics and Cosmology, vol.9, World Scientific Publishing Co., Singapore, p.212
Drew J.E., Verbunt F., 1988, MNRAS 234, 341
Frank J., King A.R., Raine D.J., 1992, "Accretion Power in Astrophysics", Cambridge University Press
Garhart M., 1992, IUE ESA Newsletter 41, 44
Hellier C., 1991, MNRAS 251, 693
Hubeny I., 1990, ApJ 351, 632
King A.R., Lasota J.P., 1991, ApJ 378, 674
Knigge C., Drew J.E., Hoare M.G., la Dous C., 1994, MNRAS 269, 891
Kuijken K., Gilmore G., 1989, MNRAS 239, 605
Lubow S.H., 1989, ApJ 340, 1064
Mateo M., Szkody P., Hutchings J., 1985, ApJ 288, 292
Nauenberg M., 1972, ApJ 175, 417
Patterson J., 1994, PASP 1086, 209
Perez M.R, 1991, IUE ESA Newsletter 38, 27
Prinja R.K., Rosen S.R., 1993, MNRAS 262, L37
Prinja R.K., Drew J.E., Rosen S.R., 1992, MNRAS 256, 219
Rutten R.G.M., van Paradijs J., Tinbergen J., 1992, A&A 260, 213
Seaton M.J. 1979, MNRAS 187, 73P
Shaviv G., Wehrse R., 1991, A&A 251, 117
Wade R.A., 1984, MNRAS 208, 381
Wade R.A., 1988, ApJ 335, 394
Warner B., 1986, MNRAS 219, 347
Warner B., Wickramasinghe D.T., 1991, MNRAS 248, 370
Woods J.A., Drew J.E., Verbunt F., 1990, MNRAS 245, 323
Woods J.A., Verbunt F., Cameron A.C., Drew J.E., Piters A., 1992, MNRAS 255, 237

This article was processed by the author using Springer-Verlag LaTeX A&A style file version 3.